Division of Informatics, University of Edinburgh

Institute of Perception, Action and Behaviour

Designing artificial ears for animat echolocation

by

Jose Carmena, DaeEun Kim, John Hallam

Informatics Research Report EDI-INF-RR-0063

Division of Informatics **September 2000**
http://www.informatics.ed.ac.uk/

Designing artificial ears for animat echolocation

Jose Carmena, DaeEun Kim, John Hallam

Informatics Research Report EDI-INF-RR-0063

DIVISION *of* INFORMATICS
Institute of Perception, Action and Behaviour

September 2000

From Animals to Animats 6, Proceedings 6th Int Conf on Simulation of Adaptive Behaviour, pp. 73-80, ed: J-A. Meyer and A. Berthoz and D. Floreano and H. Roitblat and S. Wilson, MIT Press

Abstract :

This work presents a plausible sound propagation model that can be applied to bat pinna design for echolocating animats. Previous work on artificial pinnae addressed the problem of phase cancellation in multi-reflector systems. An acoustic model inspired in a physical model of sound diffraction and reflections in the human concha, which can be scaled up to more complex surfaces, is presented. Experiments are performed in simulation as well as in the real world. RoBat, a biomimetic sonarhead mounted on a mobile robot, is used for the real world experiments. The results obtained support the plausibility of our acoustic model. A performance analysis of the reflector system with respect to the previous work is also given. Promising further work directions are also proposed.

Keywords :

Designing artificial ears for animat echolocation

Jose M. Carmena **DaeEun Kim** **John C.T. Hallam**
Institute of Perception, Action and Behaviour
Division of Informatics, University of Edinburgh
5 Forrest Hill, Edinburgh EH1 2QL, Scotland, UK
{jose,daeeun,john}@dai.ed.ac.uk

Abstract

This work presents a plausible sound propagation model that can be applied to bat pinna design for echolocating animats. Previous work on artificial pinnae addressed the problem of phase cancellation in multi-reflector systems. An acoustic model inspired in a physical model of sound diffraction and reflections in the human concha, which can be scaled up to more complex surfaces, is presented. Experiments are performed in simulation as well as in the real world. RoBat, a biomimetic sonarhead mounted on a mobile robot, is used for the real world experiments. The results obtained support the plausibility of our acoustic model. A performance analysis of the reflector system with respect to the previous work is also given. Promising further work directions are also proposed.

1. Introduction

Bats are very dynamic creatures; while flying they move their wings, head, pinnae and the nose or mouth whenever they emit. They can be divided into two broad non-taxonomic groups: broadband echolocators, or fm-bats, such as *Eptesicus fuscus*, whose cry consists of a frequency-swept chirp from around 30-90 kHz; and narrowband echolocators, or cf-bats, who emit a call where almost all the energy is in the second harmonic of a single tone (for example 83 kHz for the *Rhinolophus ferrumequinum*).

Narrowband echolocators use pinna[1] motion to alter the directional sensitivity of their perceptual systems whereas broadband listening systems (*e.g.* humans and broadband emitting bats) rely on pinna *morphology* to alter acoustic directionality at different frequencies (Walker et al., 1998). The importance of pinna motion along vertical arcs in the cf-bat for target localization in the vertical plane has been investigated with real bats (Griffin et al., 1962, Mogdans et al., 1988, Pye and Roberts, 1970). The use of this motion might be the reason that the *Rhinolophus ferrumequinum* has unusually large pinnae compared to the size of its head as can be seen in figure 1.

Figure 1: *Rhinolophus ferrumequinum* (Photos by W. Wissenbach and P. Rödl in (Nowak, 1994)).

The relationship between bats and robots arises because the sensor interpretation problems of bats, while navigating in cluttered environments such as forests, are very similar to those of mobile robots provided with ultrasonic sensors when navigating in laboratories. Moreover, the constant frequency pulse emitted by the cf-bat when echolocating is analogous to the one typically emitted by robotic ultrasonic sensors in terms of bandwidth.

Previous results in biomimetic ultrasound (Walker et al., 1998) were obtained using a bionic sonarhead consisting of one emitter and two receivers mounted on a 6 degrees of freedom head in which 6 servomotors allow panning and tilting of the neck and independent panning and tilting of each receiver. The output signals from the receivers are passed into a transputer network which hosts the signal processing module. This module models the mammalian cochlea, the output of which drives behaviours that control the motors of the sonarhead (Peremans et al., 1997).

In our work we are interested in integrating the cf-bat's sensorimotor system for obstacle avoidance and prey capture behaviours (exploiting the physical capabilities of the sonarhead) as a biological approach to ultrasonic-based navigation in mobile robots (Carmena and Hallam, 1999). For doing so we are using *RoBat*, a robotic platform composed of the sonarhead

[1] The complex convoluted external ear.

mounted on a mobile robot (figure 2).

Adding artificial pinnae to Robat will allow us to obtain cues from the sonarhead which are good for controlling the behaviour of the animat while echolocating. Next, some concepts relevant to this behaviour will be addressed (section 2). Then, a review of previous work on artificial pinnae (section 3) is presented as well as a description of the acoustic model used in this work (section 4). A comparison between these results and the results obtained in the real world is given in section 5. Finally, an analysis of the acoustic model tested on different reflector system configurations is presented in section 6, followed by some discussion in section 7.

Figure 2: RoBat: a biomimetic sonarhead mounted on a mobile robot.

2. Animal behaviour

Some aspects of bat echolocation behaviour relevant to target localisation and navigation in cluttered environments will be reviewed next.

2.1 Narrow-band 3D target localisation

It is quite interesting to see the way in which echolocators with narrow-band call structures perform target localisation. In the case of the cf-bat, this localisation is performed mostly using the information contained in a single harmonic echo. In order to calculate the target's azimuth angle with a receiver placed on each side of the head (as in bats), interaural intensity differences (IIDs) as well as interaural time differences (ITDs) can be employed.

However, how can the elevation angle be estimated? Experiments with the biomimetic sonarhead (Walker et al., 1998) showed how, by sweeping a pair of receivers through opposite vertical arcs (figure 3), dynamic cues, in the form of amplitude modulations which vary systematically with target elevation, are created (figure 4). Thus, by this arc scanning, a delay-per-degree transformation is created. This, combined with azimuth angle estimation by means of IIDs and target's range by the echo delay, provides a narrow-band echolocator with a 3D estimation of an insonified target's relative position.

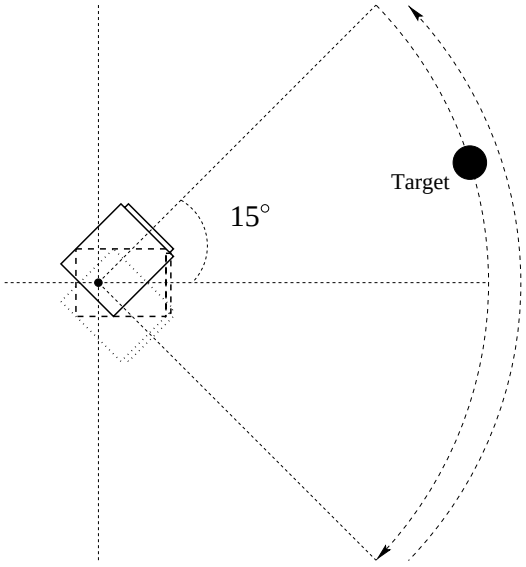

Figure 3: Side view cartoon of sonarhead's receiver performing vertical arcs for elevation angle estimation.

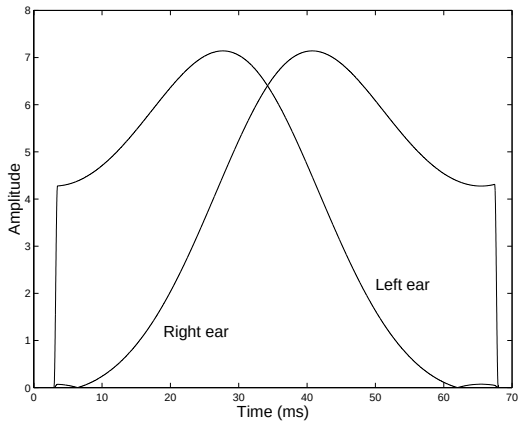

Figure 4: Delay between amplitude peaks encodes target elevation (target elevation at 6 deg.) (Walker et al., 1998).

2.2 *Obstacle avoidance and prey capture behaviours*

Regarding bat navigation, Müller and Schnitzler (1999) advance an interesting hypothesis about how bats do obstacle avoidance when tracking an insect in presence of multiple reflectors (*e.g.* foliage, tree branches, etc.). In their work, the hypothesis of an acoustic flow in which Doppler shift and echo amplitude constitute two perceptual dimensions which bats may employ for the extraction of two-dimensional crude spatial information is addressed. This information would suffice for tasks like obstacle avoidance in which high accuracy is not as necessary as in other tasks, *e.g.* prey capture.

It is well known from the literature (Schuller, 1979, Schnitzler and Ostwald, 1981) that cf-bats detect interesting properties (*e.g.* food) in echos, while navigating in cluttered environments, by the frequency shifts produced by the wing-beat cycles of fluttering insects. Such behaviour can be replicated in RoBat using computer fans[2] as targets to track (Walker, 1997).

Applying the 3D target localisation system described above to directional beacons (*i.e.* fans) as objects to track while avoiding obstacles, a sensorimotor model of prey-capture behaviour for the cf-bat is proposed (Carmena, 1999) as an adaptation of Kuc's sensorimotor model for the fm-bat (Kuc, 1994). The model is composed of a pair of controllers which apply yaw (θ) and pitch (ϕ) corrections to alter the bat's heading while pursuing a prey. For yaw corrections Kuc proposes to use IIDs which can also be applied to the cf-bat as seen in section 2.1, while for pitch corrections he proposes the use of interfrequency intensity differences (IFIDs) between the fundamental and harmonic components of the echo. This, however, can not be applied to the cf-bat because the echoes from their emitted pulses contain essentially all the energy in the second harmonic, as seen in section 1. Hence, for the cf-bat we propose to calculate pitch corrections by performing arc scanning behaviour (Carmena, 1999).

Thus, as part of our working plan, we want to improve the directional sensitivity of the sonarhead's receivers (*i.e.* maximise the angular resolution of the receiving transducers) as well as the echo amplitude by adding artificial pinnae to them. As a result of this increased discrimination, bat arc scanning and IID behaviours could be replicated in the sonarhead more successfully than using only bare transducers.

3. Previous work on artificial pinnae

First attempts in evolving bat pinna morphology (Papadopoulos, 1997, Peremans et al., 1998) used genetic algorithms to evolve simple pinna shapes for broadband echolocators because of the difficulty of designing a pinna model by an analytical approach. The evolved solutions were evaluated on a software model of the sonarhead (Walker, 1997).

The pinna was modelled by up to three disc reflectors whose position and orientation angle around the receiving transducer were determined by a genetic algorithm (GA), using a chromosome with the following structure,

$$(x_1\ y_1\ z_1\ \alpha_1\ \beta_1 \quad x_2\ y_2\ z_2\ \alpha_2\ \beta_2 \quad \ldots \quad x_n\ y_n\ z_n\ \alpha_n\ \beta_n)$$

where x,y and z are cartesian position coordinates and α, β are azimuth and elevation angles. The GA comprised a population of candidate sets of reflector positions, whose fitness was determined by simulating their effect on the acoustic signals transduced by the receiver. *2-point* crossover and a mutation rate of 0.03 were used with a population of 100. A tournament-selection scheme of size 8 wherein a set of genomes is randomly selected from the population was used. The fittest genome was selected with a given probability; if not selected, then the second best is selected with the same probability, and so on. Experiments were run for 1000 generations.

The GA (Peremans et al., 1998) was set two tasks: first, to deploy reflectors in a monaural system so as to maximise the displacement between the axes of maximal sensitivity at 30 kHz and 90 kHz (thereby allowing target elevation to be most accurately inferred from the different amplitudes of the echo at these frequencies); and second, to deploy reflectors in a binaural system to produce a maximally steep IID curve with respect to target angular position (thereby maximising the angular resolution of the binaural system and allowing the target's position to be most accurately estimated from the IID). In the binaural case, the left ear was symmetrical with the right ear, i.e. the two pinna configurations were derived from the single disposition of reflectors indicated by the GA. The results for the first experiment were reasonable, but for the second experiment no significant improvement of the IID performance could be obtained with up to three reflectors.

Such work was continued by us (Kim et al., 2000), changing the model to the narrowband (cf-bat) case and allowing up to 10 reflectors to be used by the GA (figure 5). Experiments with such a number of reflectors showed problems with phase cancellation in the received echoes. An analysis of phase cancellation suggested that more realistic pinna models, such as parabolic surfaces (in which many small reflectors would be placed around the focus point and therefore all the reflections will direct to the focus, *i.e.* the transducer) are needed for further development. However, further analysis stressed the importance of using a more accurate acoustic model before extending the work to complex surfaces. Hence, a physically plausible acoustic model is presented next.

[2] The amplitude and frequency modulations in the echo produced by the rotating blades of the fan approximate those produced by a fluttering insect (Walker, 1997).

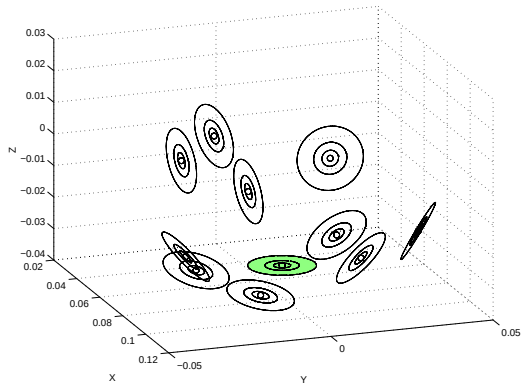

Figure 5: 10 reflector formation around transducer (shadowed) given by the GA (Kim et al., 2000).

4. Acoustic model

The acoustic models used in previous work (Kim et al., 2000, Peremans et al., 1998) used disc-shaped specular reflectors. The consideration of sound losses at the reflectors due to absorption (20% of the incident sound) in (Kim et al., 2000) was the only difference between them.

The diffraction and diffusion phenomena around the edges of the reflector discs were considered insignificant and no multiple reflections were taken into account, *i.e.* each reflector introduced one additional echo path. The reflectors' radii were constant and equal to that of the receiver, *i.e.* 26 mm.

The necessity of a more realistic model of wave propagation which could be applied to complex surfaces arises. Thus, an acoustic model inspired by a physical model of sound diffraction and reflections in the human concha (Lopez-Poveda and Meddis, 1996) is used as the starting point.

4.1 Computing reflections from finite reflectors

If we assume that the echo source is in the far field of the transducer and reflector system, the incoming echo will have planar wavefronts. (The near field case can be modelled similarly, with different assumptions about the incident waves.) The incident sound insonifies the transducer and reflectors, generating a pressure at each point $\vec{r}$ on their surfaces which is given by

$$p_0(\vec{r},t) = p_0\ e^{j(\vec{k}\cdot\vec{r}-\omega t)}$$

where $\vec{k}$ is the wave vector of the incident wave.

The total sound pressure field at the transducer is given by the direct path field, given by the equation above, and by the contributions from the reflectors. The reflector contributions can be calculated using Kirchhoff's diffraction theory (Braddick, 1965) — each point on the reflector surface is taken to be an acoustic source radiating sound in all directions. The sound pressure on any surface element of the transducer is then the integral of the contributions from each surface element of the reflector system. Using the diffraction theory model allows us to take account of the finite size of the reflector.

The reflected pressure generated at a point by a surface element on a reflector depends on the incident sound pressure, the distance to the point and the angle between the surface normal and the direction to the point. The relationship is defined by

$$dP_R(\vec{p},t) = \frac{R(d,\gamma_0)p_0(\vec{r})}{d}e^{jkd-j\omega t}ds,$$

$p_0(\vec{r},t)$ is the incident sound pressure at position $\vec{r}$ on the reflector surface (where the element ds is), d is the distance from the reflector surface element ds to the transducer (that is, $\|\vec{p}-\vec{r}\|$), k is the magnitude of the wave vector (that is, $\frac{2\pi}{\lambda}$ for a wave with wavelength λ) and γ_0 is the angle between the surface normal at $\vec{r}$ and the line joining the surface element to the point $\vec{p}$ for which the pressure is being calculated.

The directional factor for reflection is given by the reflector obliquity function (Lopez-Poveda and Meddis, 1996):

$$R(r,\gamma_0) = \frac{\cos\gamma_0}{4\pi}(-jk+\frac{1}{r}).$$

Therefore, integrating over the whole transducer surface S_T and the whole reflector surface S_R, we can obtain the total pressure contributed to the transducer which is given by the equation:

$$P_T = \iint_{S_T}\iint_{S_R}\frac{R(\|\vec{r}-\vec{p}\|,\gamma_0)p_0(\vec{r})}{\|\vec{r}-\vec{p}\|}e^{jk\|\vec{r}-\vec{p}\|-j\omega t}ds_r ds_t$$

A diagram of the plane wave model used for a transducer and reflector system is shown in figure 6. In the figure, a plane wave arriving at a surface element $\vec{r}$ of the reflector (R) insonifies a surface element $\vec{p}$ of the transducer (T) along path $\vec{p}-\vec{r}$. Note, however, that each of the reflector's surface elements will behave as an acoustic source radiating sound in all directions, not only along $\vec{p}-\vec{r}$, as explained above.

4.2 Results

A 2-dimensional adaptation of the model was tested first because of the simplicity of calculation. Figure 7 shows the curves obtained for a reflector held at different positions (0.5, 0.75 and 1 cm) and positioned along different angles (0 to 90 degrees). As expected, maximum amplitude is obtained at 45 degrees and with the reflector at the closest position of the transducer, *i.e.* 0.5 cm.

Because of the plausible results obtained with the 2D adaptation, the next step was to scale up to 3D. For

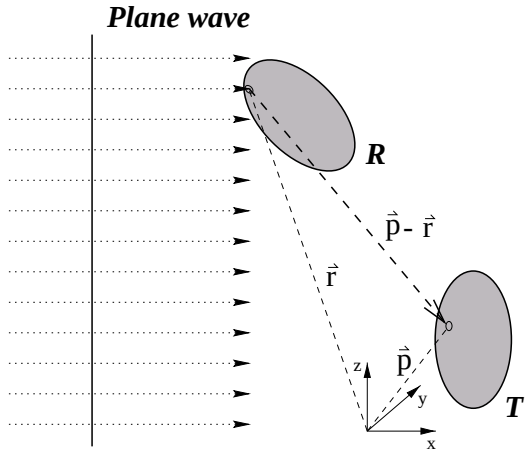

Figure 6: Plane wave model with a single reflector (R) and a transducer (T).

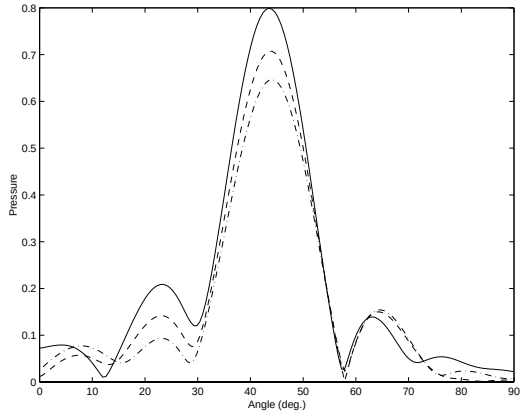

Figure 7: 2D pressure vs. reflector's effect on transducer for different angles (distances: 0.5 cm (solid), 0.75 cm (dashed), 1 cm (dashdot)).

the sake of simplicity the model was applied numerically instead of analytically. The reflector and transducer surface pressures were calculated as the sum of contributions of small divisions as an approximation to the surface integral. The division was calculated using polar coordinates, varying the radius and angle according with the number of desired surface segments. Since the larger the number of divisions, the more accurate the calculation is, 2000 vs. 800 divisions were tested, resulting in a not very significant difference as seen in the overlapping dotted curve in figure 8. Hence for the rest of the experiments 800 divisions were used.

5. Comparison with real transducer and reflector

Experiments for the simplest case, *i.e.* one reflector, were performed for a coarse evaluation of the acoustic model in the real world. From such an evaluation, evi-

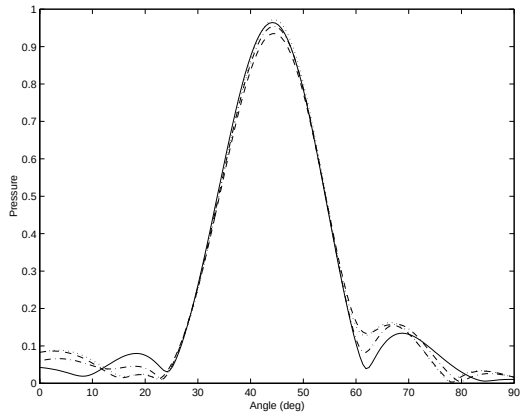

Figure 8: 3D pressure vs. 800 div. reflector's effect on transducer for different angles (distances: 0.5 cm (solid), 0.75 cm (dashdot), 1 cm (dashed)); 2000 div. reflector at 1 cm (dotted).

dence of plausibility of the simulation work could be obtained and, consequently, further complex reflector configurations might be tried.

5.1 Experimental set-up

Figure 9 shows a diagram of the experimental set-up used. The receiver to which the reflector is going to be attached is turned 90 degrees (facing the ceiling). In such a position, the bare receiver is not insonified by the echo and, therefore, a better estimation of the reflector's effect can be obtained.

Measurements were taken in increments of 7.5 degrees (from 90 to 0 degrees) with an estimated error of $\pm$ 1 degree along yaw (α) and pitch (β) angles. With respect to Cartesian coordinates a positioning error of $\pm$ 1 mm was assumed. For each measurement, 1000 consecutive pulses were sent by the transmitter to a post located 30 cm in front of RoBat. The mean value of the echo energy was calculated for each of the pulses. As seen in figure 9, the reflector's vertical distance with respect to the transducer is 1 cm because of the gap between the transducer and the grid covering it.

5.2 Results

Figure 10 shows a comparison between simulation and real echo amplitude. In the figure, the solid line represents the plane wave model, the dashed line represents the previous model (Peremans et al., 1998) and the blobs represent the mean of 1000 echo energy values.

When the real measurements were taken, the physics of the transducer-reflector configuration was not as simple as the model described in section 4. As can be seen in figure 2, each of the transducers is inside a square

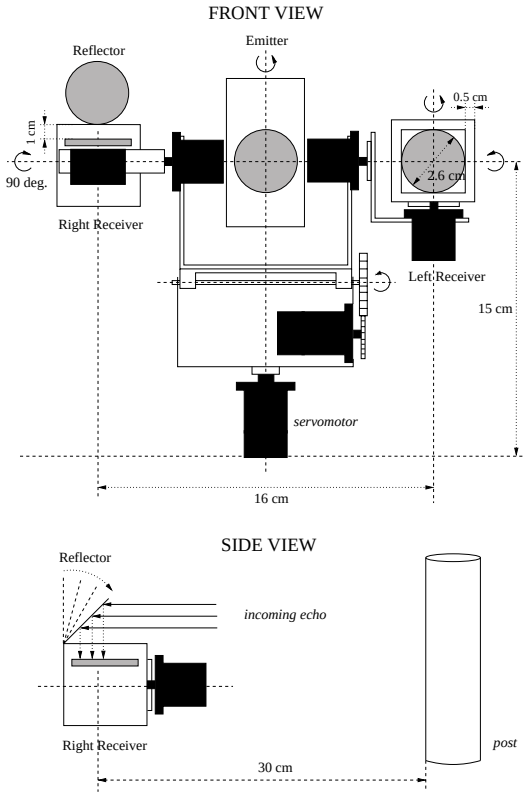

Figure 9: Experimental set-up for one reflector.

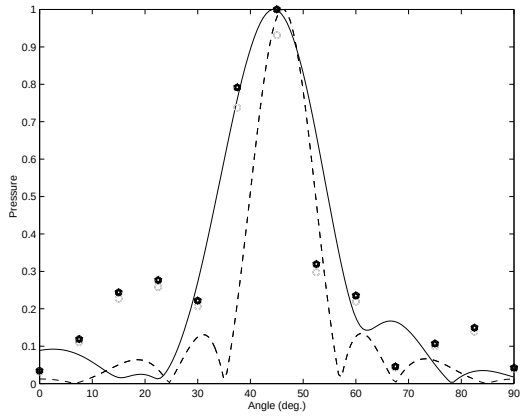

Figure 10: Results comparison between simulation work (previous model (dashed) and plane wave model (solid)) and real world (blobs).

box covered by a grid[3]. Modelling the acoustic effects of the box and grid is not straightforward and definitely mandatory for the continuation of this work. Some of the effects of this modified model can be appreciated in the interval between 10 and 30 degrees (figure 10) as a pressure offset value with respect to the simulated data. Another factor is the very low standard deviation obtained from the 13 sets (from 0 to 90 deg. in increments of 7.5) of 1000 samples whose maximum value is 0.0042 in the scale of figure 10).

Thus, this is a reasonable fit for the preliminary experimental conditions in which the measurements have been taken (sonarhead is operating in a cluttered environment) and, despite the physical differences of the real model, we can state that the data fit encouragingly well as seen in figure 10.

It is also worth mentioning the preliminary experiments done with 2 reflectors in order to see the sensitivity of multi-reflector echos to reflector position. 2 reflectors in symmetric positions were placed on the two rear corners of the receiver's box at an angle α of 45 degrees. Then, the position and orientation of one reflector, the other, and the two of them together was slightly modified, obtaining big energy variance in the final echo as a consequence of phase cancellation and shadowing effects. This suggests that for further complex experiments with several reflectors, an accurate way of positioning the reflectors in the space (*e.g.* a laser pointer based equipment) will be vital.

6. Analysis of the reflector system

In order to assess the performance of the acoustic model presented in this paper, a comparison between this model and the model used in (Peremans et al., 1998) and (Kim et al., 2000) is done (figure 11). The comparison is done using some of the reflector configurations given by the GA in (Kim et al., 2000) for 3, 5 and 10 reflectors but using the same transducer orientation as in section 5. With this orientation, because there is no direct echo reception by the transducer, it is much easier to distinguish the effects that each reflector introduces in the final wave. Then, the GA was modified for optimising the current model criteria. An evaluation of new evolved reflector configurations is presented.

6.1 Comparison between models

In any reflector system, the echo from the target will reach each reflector at a different time and therefore the path lengths from the reflectors to the receiver will be different for each case. Since the the position of the reflectors of figure 11 were evolved for the previous model, differences in performance between the two models are expected to be found.

In figure 11, the solid line is the total summation of the signals from each reflector. As can be seen, for the previous model (left column) all the reflected signals are in same phase while in the current model (right column), because of phase cancellation, the total summation is reduced. Thus, there is a clear significant difference in performance between the two models and, therefore, the model in (Peremans et al., 1998) should be replaced by

[3] This is to prevent accidental touching of the transducer (which is charged at 200 V) by the user's fingers.

the current model for any further work with complex surface systems in which spherical rather than point like waves are used.

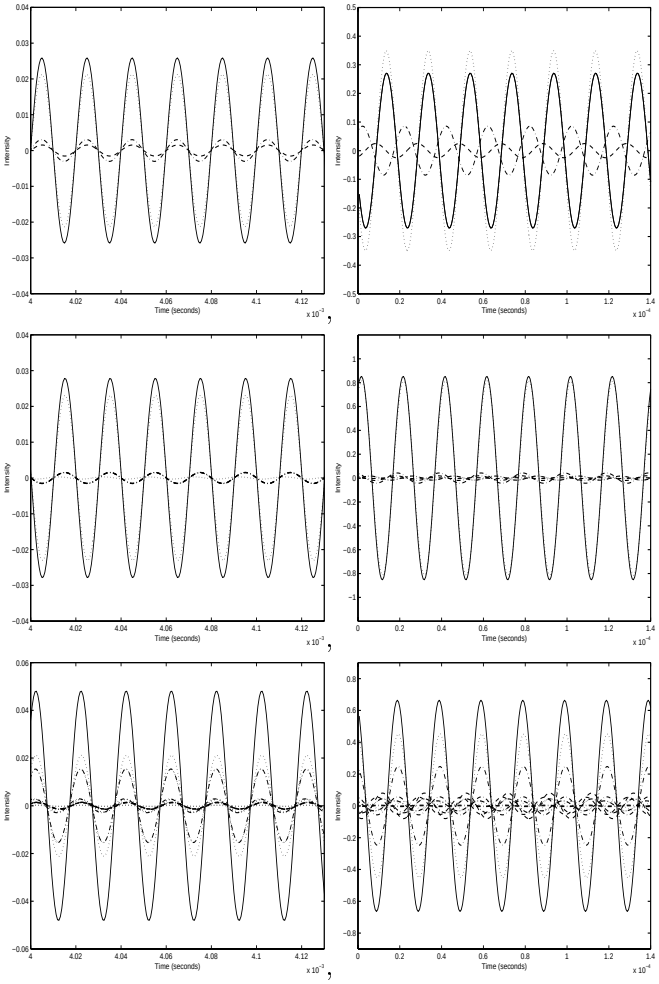

Figure 11: Comparison between previous acoustic model (left columns) and current model (right columns) for 3 (top), 5 (middle) and 10 (bottom) reflectors. Final wave (solid) is the sum of each reflector's (non solid) contribution.

6.2 Evaluation of current model

Figure 12 shows 5 (left) and 10 (right) reflector configurations (top) given by the GA for the current model and the final wave (bottom) resulting from each reflector's contribution. The important point here is the better performance of the final wave (solid line) compared to the same cases in figure 11 (right column). As seen in figure 12, the final wave has higher amplitude because of the lack of phase cancellation in both cases and, therefore, improves with respect to figure 11.

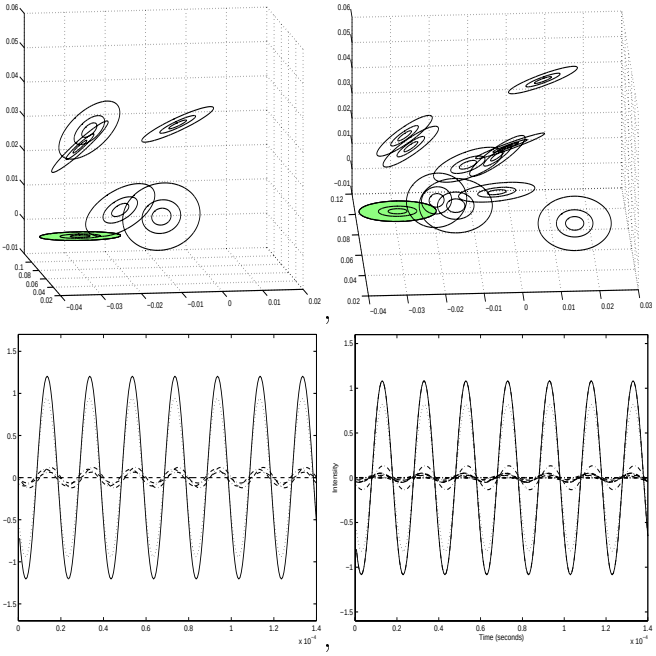

Figure 12: Evaluation (bottom) of new evolved 5 (left) and 10 (right) reflector configurations (top) for the plane wave model. Final wave (solid) is the sum of each reflector's (non solid) contribution.

7. Discussion

As said in section 3, our previous investigations addressed the importance of using a more accurate acoustic model before extending the work with complex surfaces. From the significant differences between models found in of section 6 (figure 11) and, moreover, the successful simulation results of the reflector systems evolved for the current model (figure 12), the importance of using a more realistic model of wave propagation, such as the one proposed in this work, has been demonstrated.

Regarding the experiments in the real world, the results showed the plausibility of the theoretical model despite physical differences between the real transducer and the simulated transducer as seen in figure 10. These differences, such as the transducer box with sharp edges and corners as well as the grid covering the transducer may be the cause of the energy offset found in the interval between 30 and 10 degrees.

To investigate the role of pinna shape in cf-bats, *i.e.* how pinnae account for bat behaviour as described in section 2, is the main goal of this work. For doing so, a plausible model of how sound propagates along complex and convoluted shapes as the external ear, becomes the point from which such investigations should start. At this point, evolutionary computation appears an appropriate tool for carrying on suitable experiments.

7.1 Further work

The first thing that should be done in any continuation of this work is an upgrade of the acoustic model in which the transducer's box and grid is taken into account, as suggested in section 5. Once a completed model is verified, *i.e.* by doing appropriate simple experiments in the real world as in section 5, it will be possible to proceed further.

The next step then should be setting the GA to evolve a very large number of smaller reflectors which will approximate to a surface. Long run-time experiments evolving different surfaces could be designed. At this point, replicating the spiral model of the human concha described in (Lopez-Poveda and Meddis, 1996) and also, paraboloid surfaces (figure 13) as proposed in (Kim et al., 2000) sounds a promising field to investigate.

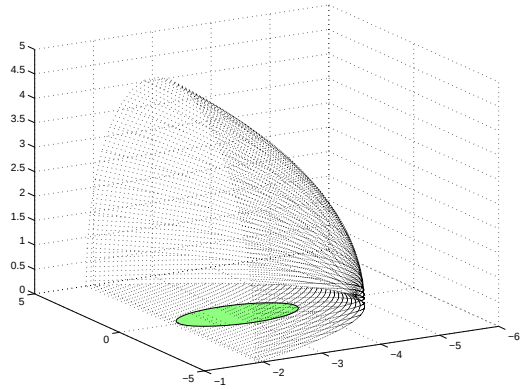

Figure 13: Example of paraboloid surface with transducer at focus position.

Acknowledgements

Jose M. Carmena is supported by the European Union TMR Network SMART2 under contract number FMRX-CT96-0052. Facilities for this work were provided by the University of Edinburgh.

References

Braddick, H. (1965). *Vibrations, Waves and Diffraction.* McGraw-Hill, London.

Carmena, J. (1999). Echolocating robots: A biological approach to mobile robot navigation. Ph.D. thesis proposal (unpublished). Division of Informatics, University of Edinburgh.

Carmena, J. and Hallam, J. (1999). A robotic platform for investigating the usage of acoustic flow in cf-bats. *138th Meeting of the Acoustical Society of America, J. Acoust. Soc. Amer.*, 106(4):2191.

Griffin, D., Dunning, D., Cahlander, D., and Webster, F. (1962). Correlated orientation sounds and ear movements of horseshoe bats. *Nature*, 196:1185–1186.

Kim, D., Carmena, J., and Hallam, J. (2000). Towards an artificial pinna for a narrow-band biomimetic sonarhead. In *ICES'2000: Third International Conference on Evolvable Systems: From Biology to Hardware*, Lecture Notes in Computer Science 1801, pages 113–122. Springer-Verlag.

Kuc, R. (1994). Sensorimotor model of bat echolocation and prey capture. *J. Acoust. Soc. Amer.*, 94(6):1965–1978.

Lopez-Poveda, E. and Meddis, R. (1996). A physical model of sound diffraction and reflections in the human concha. *J. Acoust. Soc. Amer.*, 100(5):3248–3259.

Mogdans, J., Ostwald, J., and Schnitzler, H.-U. (1988). The role of pinna movement for the localization of vertical and horizontal wire obstacles in the greater horshoe bat, *rhinolophus ferrumequinum. J. Acoust. Soc. Amer.*, 84(5):1988.

Nowak, R. (1994). *Walker's Bats of the World.* Johns Hopkins University Press.

Papadopoulos, G. (1997). Evolving ears for echolocation. Master's thesis, Department of Artificial Intelligence, University of Edinburgh.

Peremans, H., Walker, A., and Hallam, J. (1997). A biologically inspired sonarhead. Technical Report 44, Dep. of Artificial Intelligence, U. of Edinburgh.

Peremans, H., Walker, V., Papadopoulos, G., and Hallam, J. (1998). Evolving batlike pinnae for target localisation by an echolocator. In *Proceedings of the Second International Conference on Evolvable Systems: From Biology to Hardware*, pages 230–239.

Pye, J. and Roberts, L. (1970). Ear movements in a hipposiderid bat. *Nature*, 225:285–286.

Schnitzler, H.-U. and Ostwald, J. (1981). *Adaptations for the detection of fluttering insects by echolocation in horseshoe bats*, volume 56, pages 801–827. NATO ASI Series.

Schuller, G. (1979). Coding of small sinusoidal frequency and amplitude modulations in the inferior colliculus of 'cf-fm' bat, rhinolophus ferrumequinum. *Exp. Brain Res.*, 34:117–132.

Walker, V. A. (1997). *One tone, two ears, three dimensions: An investigation of qualitative echolocation strategies in synthetic bats and real robots.* PhD thesis, University of Edinburgh.

Walker, V. A., Peremans, H., and Hallam, J. C. T. (1998). One tone, two ears, three dimensions: A robotic investigation of pinnae movements used by rhinolophid and hipposiderid bats. *J. Acoust. Soc. Amer.*, 104(1):569–579.